ISSN : 0974 - 7486 Volume 12 Issue 1

Materials Science

An Indian Journal

Full Paper

MSAIJ, 12(1), 2015 [022-028]

Creep of a cast cobalt-based alloy in 3-points flexion and dependence on the applied load

Lionel Aranda, Thierry Schweitzer, Patrice Berthod*, Elodie Conrath

Institut Jean Lamour (UMR 7198), Team 206 "Surface and Interface, Chemical Reactivity of Materials", University of Lorraine, Faculty of Sciences and Technologies, B.P. 70239, 54506 Vandoeuvre-lès-Nancy, (FRANCE)

E-mail : Patrice.Berthod@univ-lorraine.fr

ABSTRACT

A cobalt-based alloy Co-25Cr-0.25C was elaborated by casting. Its microstructure was composed of a dendritic matrix and of interdendritic chromium carbides. Three parallelepiped samples were tested at 1200°C in three-points flexion under a constant load, masses leading to 10, 15 or 20 MPa as maximal stress in the middle of the sample bottom. The two first phases of creep, primary and secondary, were characterized and their dependence on the applied load studied. Laws of dependence of the deformation rate in secondary stage of creep upon the resulting maximal stress similar to what is known for tensile creep, were tried to represent this dependence. In the present case the relationship which is the most suitable is the one which corresponds to the rather low stresses.

KEYWORDS

Cast cobalt-based alloy;
Points flexion;
High temperature;
Creep deformation.

INTRODUCTION

Besides high temperature oxidation and corrosion the main destructive phenomenon for alloys and superalloys used in hot conditions with applied stresses is creep deformation[1]. This progressive deformation which is induced by a constant applied stress appears at high temperature. It is generally considered that creep becomes significant when a sufficient stress is applied at an absolute temperature higher than half the absolute solidus temperature of the alloy. Creep is a viscous-plastic deformation which can occur for different modes of mechanical solicitation: traction, compression, flexion, torsion… Generally it starts with a fast deformation which thereafter progressively decelerates. During this first part of creep deformation (primary creep) the dislocations become very numerous and the Franck's network finishes stabilizing. Thereafter, the alloy continues to deform with a low and constant rate (secondary creep), a stage which is generally the longest one. During this secondary stage of creep dislocations continue to reach the grain boundaries where they accumulate to finally promote the start of local grains debonding. Deformation accelerates again (tertiary creep) to lead to the final rupture (if the alloy is solicited in traction, flexion or torsion). The applied stress and the temperature have both a significant effect on each of the three stages of creep, as schematically illustrated in Figure 2 and the laws of dependence need to be known.

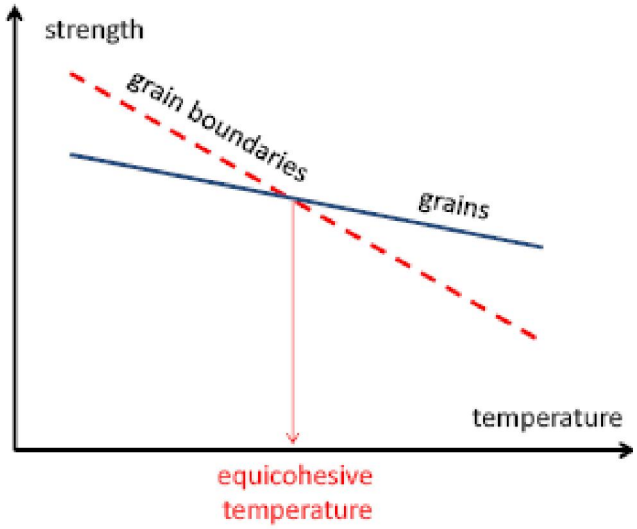

Figure 1 : Scheme reminding the mechanical superiority of grains by comparison to grain boundaries at elevated temperature

Concerning the effect of temperature, the deformation rate during the secondary stage of creep generally obeys an Arrhenius law, which can be written as (Eq.1). For a given temperature and when the applied stress is not very high the secondary creep deformation rate depends on stress according to (Eq. 2). This is according to (Eq. 3) when the applied stress is particularly high.

$$\frac{d\varepsilon_{II}}{dt} = C^{st} \times e^{\frac{-Q}{R \times T}} \quad (1)$$

$$\frac{d\varepsilon_{II}}{dt} = C^{st} \times \sigma^{n} \quad (2)$$

$$\frac{d\varepsilon_{II}}{dt} = C^{st} \times e^{(\propto \times \sigma)} \quad (3)$$

where ε_{II} is the deformation during the secondary stage of creep, C^{st} are constants, Q is the activation energy (J/mol; Q depends on the constant applied stress), R the constant of the state law of perfect gases (8.314 J/mol/K), and n and α coefficients.

Among the more creep-resistant refractory alloys and superalloys there are the cobalt alloy's family[2]. The best ones are the cast ones. indeed the latter generally present coarse microstructures which are more favourable than the fine ones when the service temperature is higher than the equicohesive temperature beyond which the grain strength is higher than the grain boundaries strength[3], as schematized in Figure 1.

In contrast with the best nickel-based superalloys, {single crystal}-constituted and efficiently reinforced by intermetallic particles (gamma prime γ'), cobalt-based alloys must be strengthened by solid solution or by carbides. Generally they do not contain aluminium but chromium with high contents to resist high temperature oxidation and hot corrosion[5,6].

In this work the creep behaviour at high temperature of a simple cobalt based-alloy which can be as a specimen of its family with its 25wt.%Cr and 0.25wt.%C, was studied in order to specify the effect of the level of the stress applied on the two first parts of creep, the primary stage and the secondary one. This may be of interest for prediction purpose.

EXPERIMENTAL DETAILS

Elaboration of the alloy

The alloy under study was preliminarily elaborated by foundry. Parts of pure cobalt, pure chromium and graphite (Alfa Aesar, purity better than 99.9%) were weighed to prepare a 40g-ingot with the Co(bal.)-25Cr-0.25C (wt.%) chemical composition. The apparatus used for the elaboration was a CELES furnace allowing the heating by high frequency (about 100 kHz) induction (Foucault currents and Joule effect) of the elements. Heating, melting and cooling/solidification were achieved under 300millibars of pure argon in a water-cooled copper crucible isolated from air by a silica tube. The obtained ingot was cut in order to obtain a sample for the microstructure examinations and three samples for the creep tests.

Sample for metallographic observations

The part of alloy destined to microstructure observations was embedded in a cold resin mixture (ESCIL), ground with SiC papers from 240 grit to 1200 grit, ultrasonically washed, polished with textile disk enriched with 1µm diamond suspension. The microstructure was observed using a Scanning Electrons Microscope (JSM 6010LA of JEOL) in Back Scattered Electrons mode (SEM in BSE mode).

Samples for creep tests

The parts destined to the creep tests were parallel-

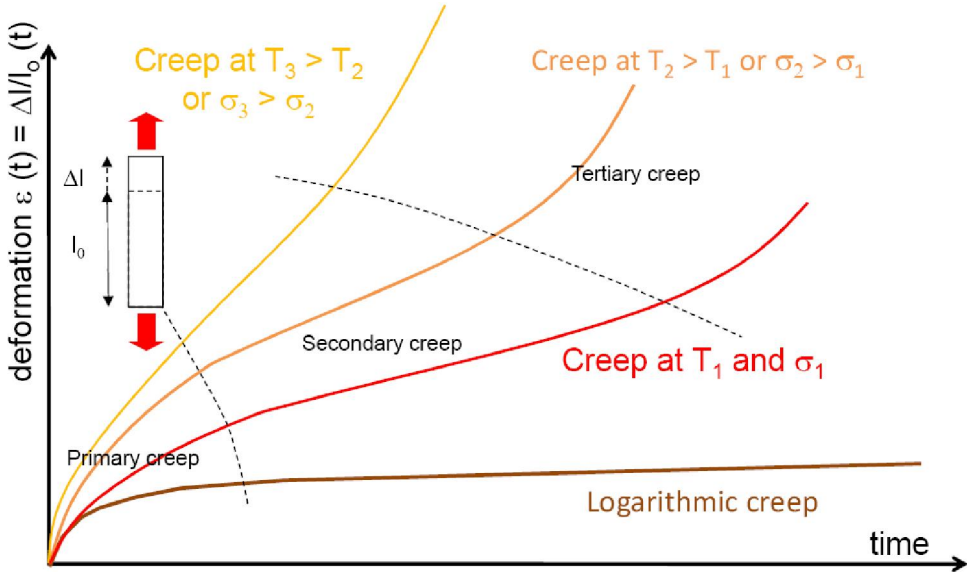

Figure 2 : General shape of a creep deformation curve and effects of temperature and stress (case of tensile solicitation)

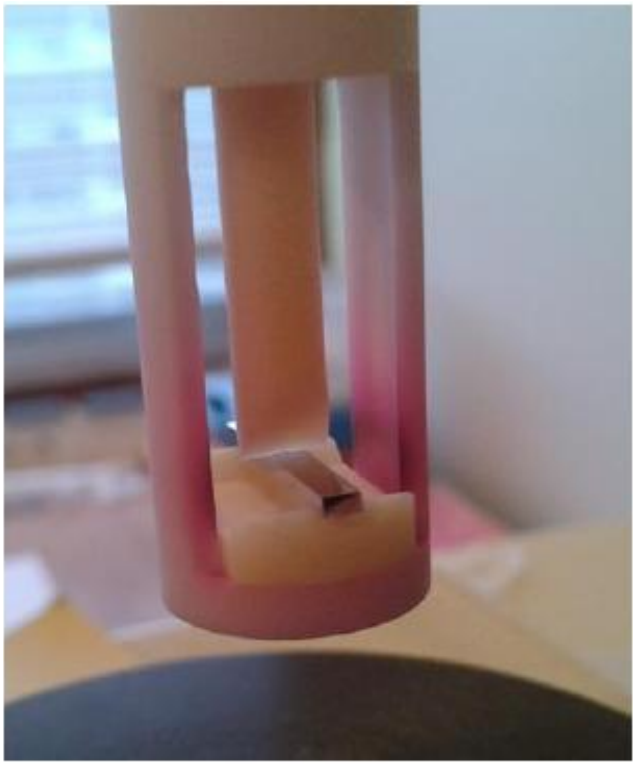

Figure 3 : Photograph of the alumina apparatus allowing the dilatometer performing bending tests under constant load at high temperature

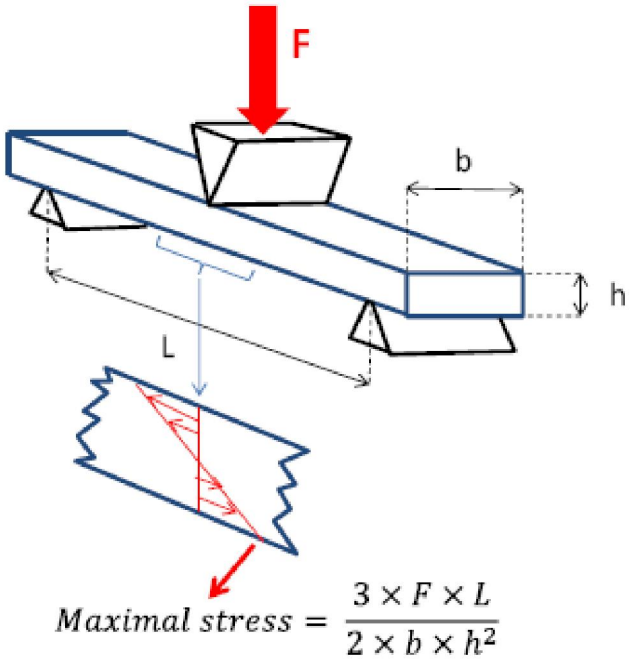

Figure 4 : Scheme representing the stress distribution in the thickness of the sample just under the upper support; value of the resulting maximal tensile stress.

epipeds. Their average dimensions were 15mm (length) × 2mm (width) × 1mm (thickness). They were polished all around with 1200 grit papers. The bottom 15mm (length) × 2mm (width) face was further polished with the {1µm diamond}-enriched disk in order to obtain a mirror-like state. This will allow microstructure observation before test. This may permit having useful elements to eventually explain curious behaviour (detection of eventual microstructure defects where the stress will be maximal).

Realization of the creep tests

The apparatus used for performing the creep tests is a dilatometer (SETARAM TMA 92-16.18) especially equipped (Figure 3). The normal alumina-made

device for thermal expansion measurements was removed and replaced by an alumina-made special device which allows performing 3 points bending tests.

The space between the two bellow supports was 12mm wide and the upper support was centred relative to the bellow support. An argon flow allowed inerting the chamber. The load (a dead mass + an electronic complementary mass) was applied by the upper central support before heating. Heating was then started (heating rate: +20°C/min) was performed until reaching 1200°C. After a 48 hours dwell the cooling down to ambient temperature was done at -20°C/min.

The loads which were applied were calculated in order to obtain, in the middle of the bottom of the samples, a maximal tensile stress of 10 MPa (load: about 110g), 15 MPa (load: about 150g) or 20 MPa (load: about 200g).

The progressive downwards movement of the upper support was recorded and the results plotted versus time. The obtained curves were analysed, in the present state, after derivation (deformation rate versus time). Further analysis was also done after derivation and smoothing (each value replaced by the average value of the ten neighbour ones), in order to distinguish the primary creep and the secondary creep from one another. The duration of the primary creep as well as the total deformation achieved during this first stage, and the average constant rate of deformation during the secondary creep, were specified. They were studied with regards to the maximal stress resulting from the applied load.

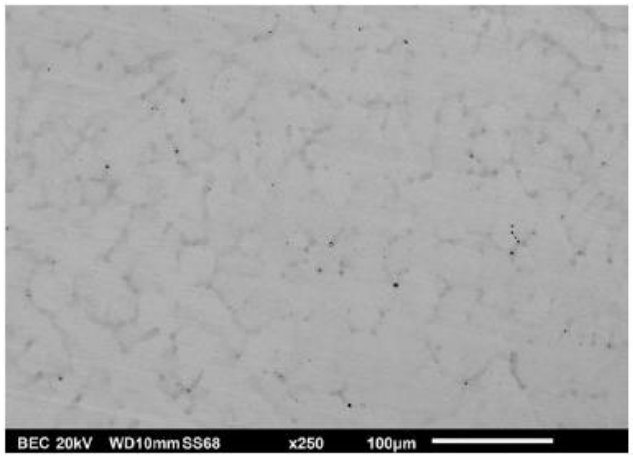

Figure 5 : Microstructure of the Co (bal.)-25Cr-0,25C alloy (wt.%); SEM micrograph in BSE mode

RESULTS

The microstructure of the alloy before creep bending test is illustrated by the micrograph presented in Figure 5. One can see the dendritic character of the matrix and the chromium carbides having precipitated in the interdendritic spaces where segregation occurred during solidification are also visible.

The samples were photographed after test. They are shown in Figure 6 in which one can see that the movement of the central upper support was logically more important for a higher applied load. One can notice that oxidation occurred during the test. Indeed pure argon always contains very low O_2 quantities. These ones are sufficient to provoke oxidation, especially at a so high temperature as 1200°C and for a rather long time (two days). The three samples were wholly cov-

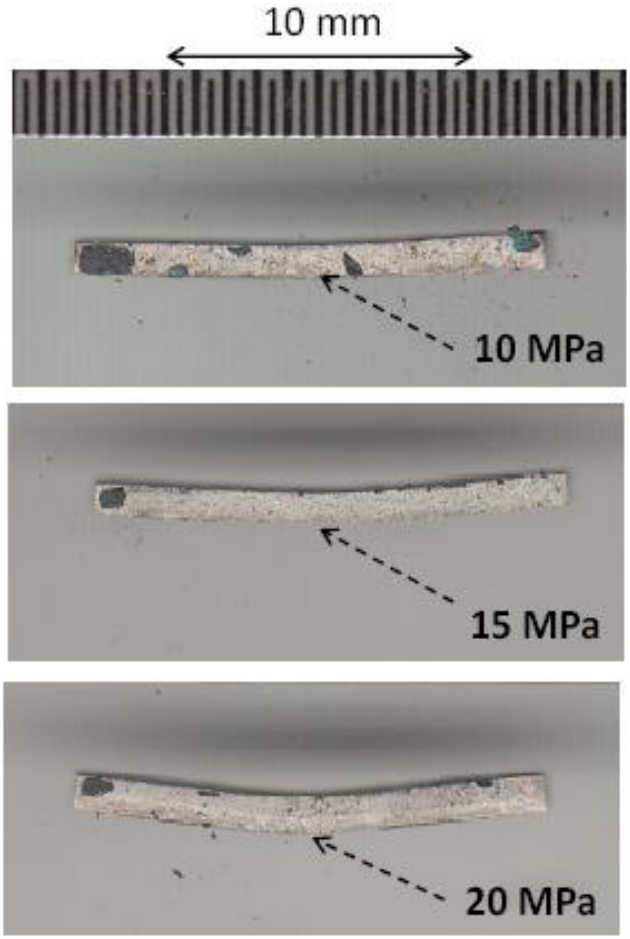

Figure 6 : Macrographs of the deformed samples after creep for 48 hours at 1200°C (10 MPa, 15 MPa and 20 MPa) are the stresses resulting from the loads applied in the bottom face of the samples at half length)

ered by oxide (mainly chromia as revealed by its green colour) but the main part of this oxide fell down notably during the exiting of the sample and its handling.

The measurements are presented in Figure 7 in which the three creep curves are plotted together. Since the mechanical solicitation mode is flexion and not traction or compression, it is not a relative deformation which is plotted versus time but simply the movement of the central upper support, thus in micrometers (µm) and not in %. Clearly, the higher the applied stress, the faster the deformation of the sample. In the three cases (10 MPa, 15 MPa and 20 MPa) the curve presents a primary creep part and a secondary creep part. The primary creep was then finished or almost finished before reaching the 46 hours and it was more or less partly replaced by the secondary creep.

The deformation was derived versus time in order to get new curves on which the transition from the primary creep to the secondary creep may be more obvious. On these curves, which are presented in Figure 8, one can effectively clearer see after which time the deformation rate can be considered as constant.

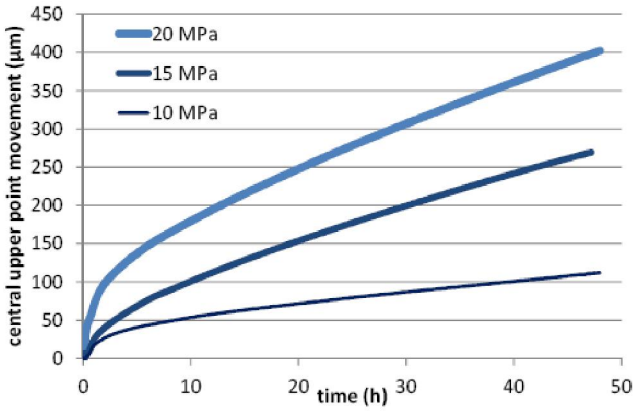

Figure 7 : The three creep-deformation curves plotted together

These derived curves allowed specifying the time separating the primary phase and the secondary phase, which allowed to draw the regression straight line from the good time to the end of experiment since no tertiary creep phase obviously took place before 48 hours. The slopes of these three straight lines are given in the deformation curves presented in Figure 9 in which the secondary creep is delimited.

General commentaries

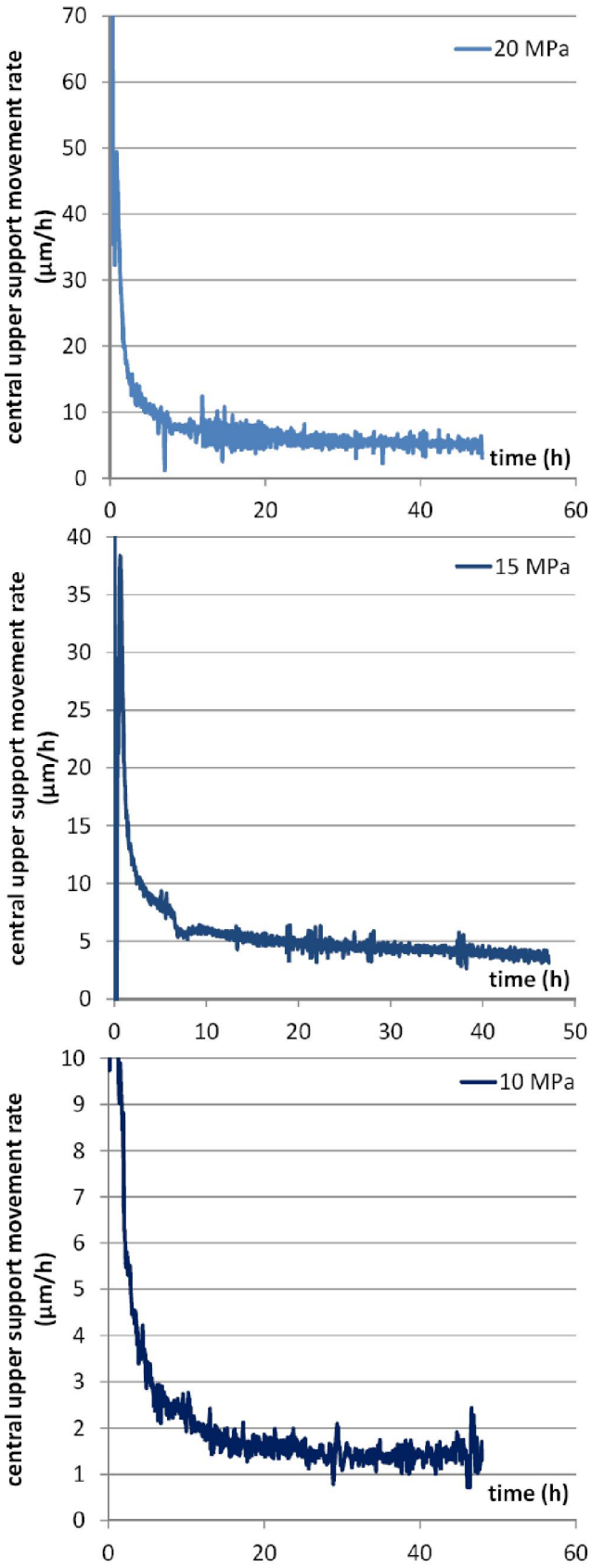

Figure 8 : The three creep curves after derivation versus time

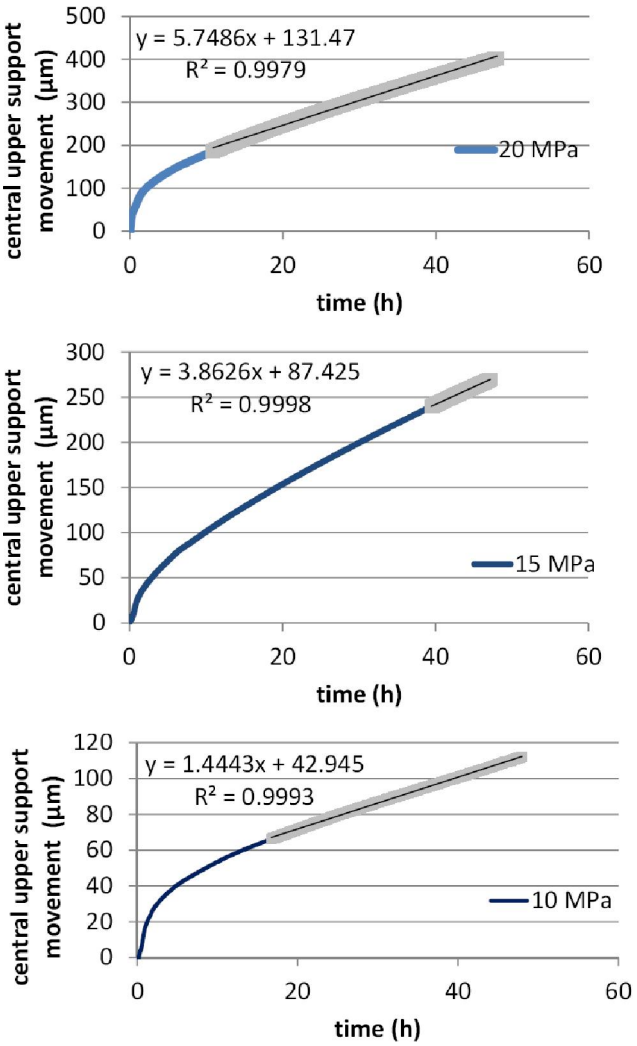

Figure 9 : The deformation curves with the delimitation of the secondary creep phase and the equation of the regression straight line giving the secondary creep deformation rate (the slope)

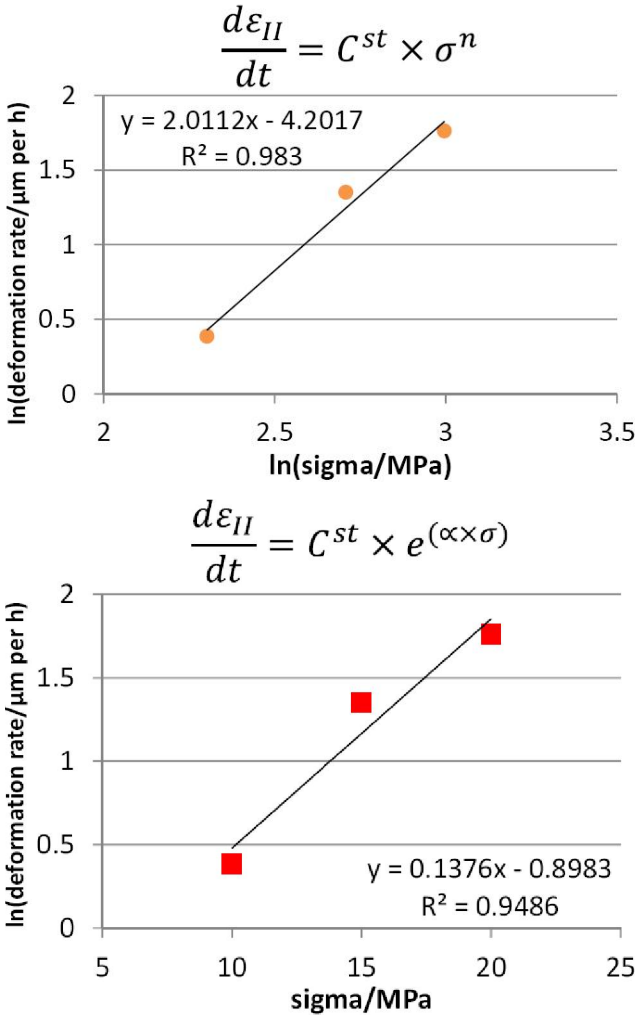

Figure 10 : Plot of the deformation rate in secondary creep phase according to Eq. 2 (top) and Eq. 3 (bottom)

These three creep tests led to many data which can be piled up in TABLE 1. One can see that the higher the maximal stress:

- the shorter the primary creep duration
- the more important the final deformation at the primary → secondary transition
- the faster the constant deformation rate during the secondary phase of creep.

These observations are the ones generally done for the deformation rate in traction (in % / h and not simply in µm here), and which were reminded above in Figure 2. It can be interesting to examine whether the deformation rate during the secondary creep phase obeys a law similar to the ones known in case of traction-creep and reminded above (by Eq. 2 and Eq. 3). The Neperian logarithm of the deformation rate is then plotted versus the Neperian logarithm of the resulting maximal stress (upper graph) and versus this later stress itself (bottom graph) in Figure 10. One can see that the three points are almost aligned in both cases, perhaps more in the first case than in the second case. By considering the first graph the slope, about 2, should be the value of "n" which is usually comprised between 3 and 8 in case of "dislocation creep" and close to 1 in case of "diffusion creep". By considering the second case, the α coefficient should be equal to 0.138 MPa^{-1}. These two rather good alignments of the three points in both cases let think that, despite the present case is far from a traction-creep situation with a maximal stress existing only locally in contrast with a whole section, similar relationships as Eq. 2 and Eq. 3 may be written for this type of deformation (which is not relative and which results from

TABLE 1 : Data resulting from the exploitation of the three creep curves

Creep deformation kinetic for a resulting stress equal to	Primary stage		Secondary stage (μm/h)	
	Duration (h)	Final deformation (μm)	Slope of theregression straight line	Rate (average value after derivation)
20 MPa	10.85	186	5.75	5.82
15 MPa	14.02	123	3.86	3.86
10 MPa	16.73	1.61	1.44	1.47

a much more complex mechanical phenomenon). Furthermore the values obtained for the coefficients existing in the two laws let think that 1200°C is for this alloy intermediate between the dislocation creep and diffusion creep temperatures, and the 10 to 20 MPa of resulting maximal stress is intermediate between low stress and high stress.

CONCLUSION

Even if bending tests are less informative than tensile tests they may give some indication about the tensile strength of materials but, it is true, very locally in 3–points configuration. Here this was more precisely about the creep resistance that the apparatus adapted to the dilatometer allowed to observe the strength of the studied cobalt alloy. It was not the local viscous-plastic tensile strain which was measured here but simply the progressive downwards movement of the central upper support. However one observed the same succession of principal creep phases as in high temperature constant tensile solicitations: primary phase then secondary phase. By characterizing these ones in terms of duration, whole deformation amount and constant deformation rate, one encountered the same consequences of an increasing stress as the ones usually observed in creep tensile tests. Furthermore the deformation rate during the secondary creep seems obeying the same laws as well known in tensile tests. This may probably allow predictions for interpolated values of load and of not far extrapolated ones.

Further work can be now performing similar tests for the same alloy, but longer enough to observe also the secondary → tertiary creep transition (and may be rupture if this one occurs before the deformed sample reaches the bottom of the apparatus). One can also think to higher temperature for studying the dependence of the deformation upon this other main parameter.

REFERENCES

[1] C.T.Sims, W.J.Hagel; The Superalloys, John Wiley and Sons, New York, **(1972)**.

[2] A.M.Beltram, C.T.Sims, N.S.Stoloff, W.C.Hagel; Superalloy II – High temperature materials for aerospace and industrial power, John Wiley, 135 **(1987)**.

[3] E.F.Bradley; Superalloys: A Technical Guide (1st Edition), ASM International, Metals Park, **(1988)**.

[4] M.J.Donachie, S.J.Donachie; Superalloys: A Technical Guide (2nd Edition), ASM International, Materials Park, **(2002)**.

[5] P.Kofstad; High Temperature Corrosion, Elsevier applied science, London, **(1988)**.

[6] J.Young; High temperature oxidation and corrosion of metals, Elsevier, Amsterdam, **(2008)**.